Oxidative precipitation of Mn(II) from cobalt leach solutions using dilute SO₂/air gas mixture

by N. Mulaudzi*†, and T. Mahlangu†

The work published in this paper is in partial fulfilment of an M.Eng Metallurgical Engineering thesis from the University of Pretoria

Synopsis

The use of SO₂/air gas mixtures as an oxidant to precipitate Mn from Co(II) leach liquors was investigated. The effects of SO₂/air ratio, pH and temperature on Mn precipitation were evaluated. It was found that the use of SO₂/air gas mixtures resulted in significantly higher Mn precipitation kinetics compared to using air or pure O₂ alone.

The SO₂/air ratio was varied from 0% to 6% SO₂ (v/v) in air and similar Mn removals were achieved at 0.75% to 3% SO₂ at pH 3. The solution pH was varied from pH 2 to pH 4; Mn precipitation did not increase considerably from pH 2 to pH 3, but increased significantly at pH values higher than pH 3. Cobalt co-precipitation also increased as pH increased, with 1% Co co-precipitation at pH 3. An increase in temperature from 30°C to 60°C also increased Mn precipitation and 100% Mn precipitated at 50°C. Cobalt co-precipitation also increased significantly with an increase in temperature. An activation energy of 25 kJ/mol was calculated from the Arrhenius plot, which is an indication that the precipitation reactions were both chemically and diffusion controlled.

XRD analysis showed that Mn precipitated in the form of Mn₂O₃ instead of MnO₂ that was predicted from thermodynamic data. SEM and XRD analysis also revealed that the precipitate consisted mainly of gypsum or bassanite (99%), with the Mn containing phase (< 1%) distributed within the gypsum phase. The co-precipitated Co reported to the Mn phase.

Keywords: manganese precipitation; SO₂/O₂ gas mixtures; cobalt solutions.

Introduction

Manganese occurs in most cobalt, copper, nickel and zinc ores as an impurity, which reports to the leach solution when the valuable metal is leached from the ore. The leach liquor obtained from these ores often must be purified to an extent before the valuable metal is recovered either by electrowinning or precipitation.

Some Mn(II), approximately 2–5 g/ℓ, is desired in Co(II) electrowinning in order to form a protective MnO_2 layer on the lead anode surface, which limits corrosion of the anode. Consequently, control of the manganese concentration in the advance electrolyte is not as stringent if present at low concentrations. However, if the valuable metal has to be recovered by precipitation of a relatively high quality cobalt salt, the level of Mn(II) in the purified leach solution should be extremely low, in the range of 10 mg/ℓ or less.

There are various methods that are used for the removal of Mn from leach solutions, namely: ion exchange, solvent extraction and precipitation. Precipitation of manganese is a cheaper and simpler alternative compared to solvent extraction and ion exchange. Several research studies have been undertaken to investigate the use of SO_2/O_2 gas mixtures as an oxidant to precipitate Mn from Zn(II), Co(II) and Ni(II) leach liquors (Menard *et al.*, 2007; Zhang *et al.* 2002; Zhang *et al.*, 2007). The use of SO_2/O_2 or SO_2/air gas mixtures as an oxidant is attractive because it is cheaper compared to using other strong oxidants such as ozone and hydrogen peroxide. The running costs for precipitating metals with SO_2/O_2 or SO_2/air gas mixtures can be reduced by using scrubbed SO_2 from the sulphide ore roasting operations if the plant is processing a sulphide ore.

The subject of this paper was to investigate ways to optimize the precipitation of manganese from cobalt leach solutions to produce a less contaminated cobalt solution from which cobalt can be recovered as a high quality precipitate. The effects of the SO₂/air ratio, pH and temperature were investigated to determine the optimum conditions for maximum Mn precipitation with reasonably low cobalt losses (<1%). The use of pure oxygen instead of air in the gas mixture was also compared.

* Hydrometallurgy Division, Mintek, South Africa.
† Department of Materials Science and Metallurgy, University of Pretoria, Pretoria, South Africa.

Oxidative precipitation of Mn(II) from cobalt leach solutions using dilute SO_2

Theory

Thermodynamic considerations

The possible reactions of Mn and Co can be predicted from the Pourbaix diagram, Figure 1, which illustrates the regions where the various species that may form predominate. Oxidative precipitation of Mn(II) to MnO_2 becomes thermodynamically feasible if the redox potential of the system rises above that of the MnO_2/Mn(II) line, represented by the long red line from pH 0 to pH 7. Precipitation of Mn(II) as Mn_2O_3 becomes thermodynamically possible at pH > 5, represented by the region between the two parallel red lines from pH 5 to pH 7.

In the pH range investigated, namely pH 2 to pH 4, Co(II) is expected to remain in solution at redox potentials below the Co_3O_4/Co(II) line as indicated by the purple line in Figure 1. If the redox of the system rises above this line, oxidative precipitation of Co(II) as Co_3O_4 becomes thermodynamically feasible. The experimental conditions should therefore be controlled such that the redox potential does not exceed Co(II) oxidation potentials at all pH values.

Solubility of sulphur dioxide and oxygen

Sulphur dioxide is more soluble in water compared to oxygen. The solubility of SO_2 and O_2 at 25°C has been reported to be 94.1 g/ℓ and 0.04 g/ℓ respectively (Brandt *et al*. 1994). Therefore in the SO_2/air system one would expect the mass transfer of O_2 to be limiting due to its low solubility compared to gas. Several authors have reported that O_2 mass transfer is limiting for oxidative precipitation of Mn(II) and Fe(II) using SO_2/O_2 gas mixtures (Menard *et al*. 2007; Zhang *et al*. 2000). Zhang *et al*. (2000) also reported that an increase in temperature resulted in a decrease in the optimum SO_2/O_2 ratio due to reduced O_2 solubility as temperature increases.

The solubility of SO_2 is known to be pH dependent; the SO_2 uptake in water droplets was found to decrease with decreasing pH. As a result SO_2 is less soluble in acidic water (Brandt *et al*. 1994). The speciation of S(IV) oxides in water also varies with pH as illustrated in Figures 2 and 3. Different S(IV) species are known to have different reactivities, with SO_3^{2-} reported to be 20–40 times more reactive than HSO_3^-

(Brandt *et al*. 1994). In addition Brandt *et al*. (1994) cited Ali *et al*. who reported that for the oxidation of S(IV) by a Co(III) complex, the reactivity of the S(IV) species was in the following order: SO_3^{2-} > HSO_3^- > .H_2O; where SO_3^{2-} was reported to be 16 times more reactive than HSO_3^- and HSO_3^- was 53 times more reactive than $SO_2.H_2O$. It has been reported that pH affects the stability of the produced transition metal complexes (Brandt *et al*. 1994). Zhang *et al*. (2000) reported that the optimum SO_2/O_2 ratio was dependent on pH and it has also been shown that an increase in pH increased Mn precipitation kinetics (Zhang *et al*. 2002).

In the pH range investigated, pH 2 to pH 4, the dissolved is expected to be mainly in the form of HSO_3^- as indicated in Figure 2. The Pourbaix diagram in Figure 3 also shows that HSO_3^- is the predominant S(IV) species at pH 2 to pH 4 at relatively low potentials.

Proposed oxidation mechanism

A radical mechanism has been proposed for the autoxidation of S(IV) by O_2 in the presence of certain transition metal ions,
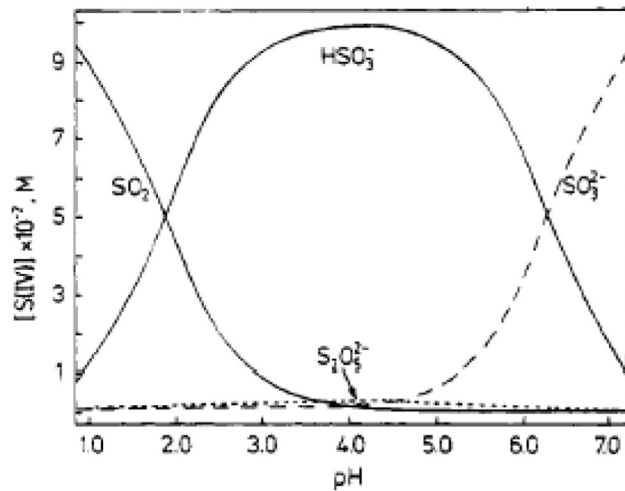

Figure 2—Distribution of sulphur(IV) oxide species as a function of pH (5 x 10^{-2} M $Na_2S_2O_5$, 25°C) (Brandt *et al*. 1994)
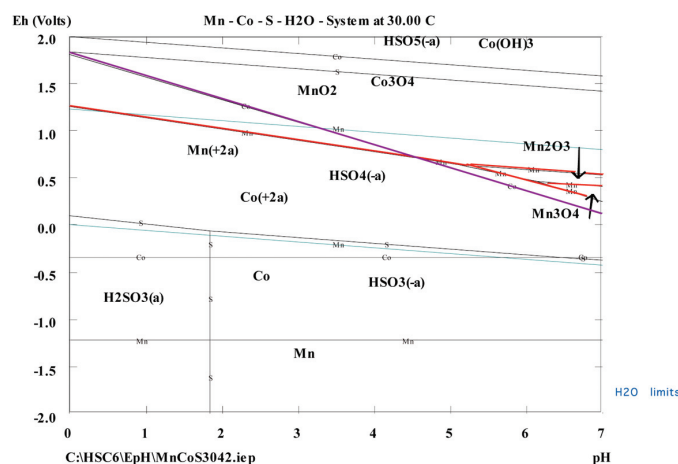

Figure 1—The Pourbaix diagram for 2 g/ℓ Mn(II), 6.5 g/ℓ Co(II) and 4.8 g/ℓ S(IV) at 30°C and 1 atm as predicted by the HSC thermodynamic model

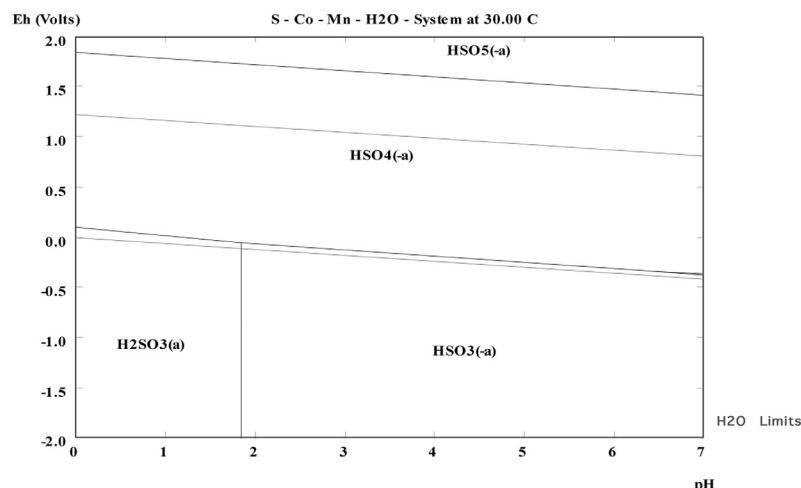# Oxidative precipitation of Mn(II) from cobalt leach solutions using dilute SO$_2$ air

Figure 3—Pourbaix diagram for 4.8 g/l S(IV) at 30°C and 1 atm as predicted by the HSC thermodynamic model

namely: Cu(II), Fe(III), Ni(III), Co(III) and Mn(IV) (Brandt *et al*. 1994; Berglund *et al*. 1994; Das *et al*. 1999). The proposed mechanism results in the net oxidation of the transition metal ions as well as the oxidation of S(IV) species. The mechanism proposed by Berglund *et al*. requires tetravalent metal ions to react with the S(IV) species in order to form a complex, which is known to initiate the radical chain reactions. Brandt *et al*. suggested that it was possible to form a similar complex with the divalent metal ion and the S(IV) species, which also gives rise to radical formation. Huie *et al*. (1987) reported that ultraviolet rays were required to initiate radical formation.

The mechanisms proposed by the various authors are similar; Brandt *et al*. studied the mechanism using computer simulations and derived it as indicated by Equations [1] to [6].

Initiation reactions

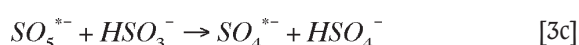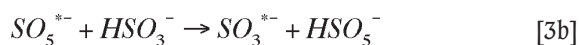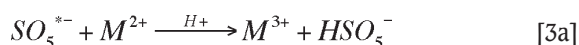$$M^{3+} + HSO_3^- \rightarrow MSO_3^+ + H^+ \qquad [1a]$$

$$MSO_3^+ \rightarrow M^{2+} + SO_3^{*-} \qquad [1b]$$
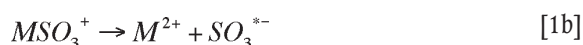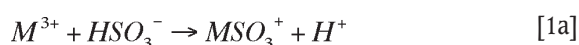
In the presence of O$_2$, the SO$_3$*- radical reacts with O$_2$ to form the peroxymonosulphate radical, SO$_5$*-, which is understood to control the redox cycle.

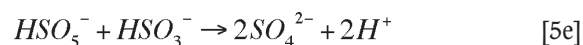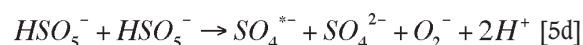$$SO_3^{*-} + O_2 \rightarrow SO_5^{*-} \qquad [2]$$

Propagation reactions

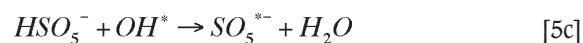SO$_5$*- is a more reactive oxidant than O$_2$ and is believed to oxidize the divalent transition metal ions and the S(IV) as follows:

$$SO_5^{*-} + M^{2+} \xrightarrow{H+} M^{3+} + HSO_5^- \qquad [3a]$$

$$SO_5^{*-} + HSO_3^- \rightarrow SO_3^{*-} + HSO_5^- \qquad [3b]$$

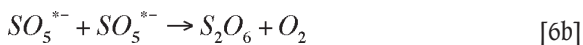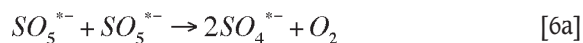$$SO_5^{*-} + HSO_3^- \rightarrow SO_4^{*-} + HSO_4^- \qquad [3c]$$

The SO$_4$*- radical is known to be a very strong oxidant with a standard reduction potential of 2.43 V vs. SHE, and is therefore expected to rapidly oxidize sulphite and transition metal ions (Das *et al*. 1999). The produced SO$_4$*- radical can participate in oxidation reactions as follows:

$$SO_4^{*-} + M^{2+} \rightarrow M^{3+} + SO_4^{2-} \qquad [4a]$$

$$SO_4^{*-} + HSO_3^- \rightarrow SO_3^{*-} + HSO_4^- \qquad [4b]$$
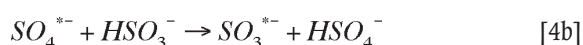
The HSO$_5^-$ anion formed by the oxidation of S(IV) and M^{2+} by the SO$_5$*- radical, together with the SO$_5$*- radical open various reaction pathways. These reaction pathways may influence both the decomposition process and the product formation as indicated by Equations [5] to [6]

$$HSO_5^- + M^{2+} \rightarrow M^{3+} + SO_4^{*-} + OH^- \qquad [5a]$$

$$HSO_5^- + M^{2+} \rightarrow M^{3+} + SO_4^{2-} + OH^* \qquad [5b]$$

$$HSO_5^- + OH^* \rightarrow SO_5^{*-} + H_2O \qquad [5c]$$

$$HSO_5^- + HSO_5^- \rightarrow SO_4^{*-} + SO_4^{2-} + O_2^- + 2H^+ \qquad [5d]$$

$$HSO_5^- + HSO_3^- \rightarrow 2SO_4^{2-} + 2H^+ \qquad [5e]$$

Termination reactions

$$SO_5^{*-} + SO_5^{*-} \rightarrow 2SO_4^{*-} + O_2 \qquad [6a]$$

$$SO_5^{*-} + SO_5^{*-} \rightarrow S_2O_6 + O_2 \qquad [6b]$$

The recombination of SO$_4$*- was proposed to be unlikely due to excess S(IV) and M^{2+} and was therefore not included in the reaction scheme (Brandt *et al*. 1994).

Studies conducted by Das *et al*. (1999) on the reduction potentials of the SO$_3$*- and SO$_5$*- radicals by pulse radiolysis revealed that the potential of the radicals was dependent on pH as indicated in Figure 4. This indicates that redox reactions that involve the radicals shown in Figure 4 are dependent on the pH of the system.

Reaction stoichiometry

The overall reactions for oxidative precipitation of Mn with SO$_2$/O$_2$ gas mixtures are illustrated by Equations [7] to [10]. Mn is expected to precipitate as MnO$_2$ at pH values below pH 7 and high redox potential; and as Mn$_2$O$_3$ in the pH range of 5 to 7 at relatively high redox potential values below those required for MnO$_2$ precipitation (see Figure 1).

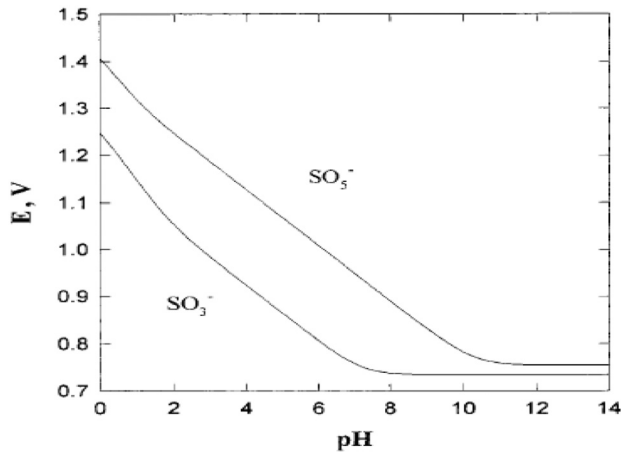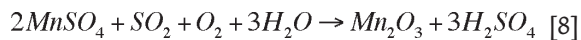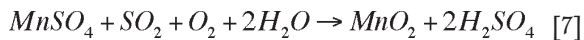# Oxidative precipitation of Mn(II) from cobalt leach solutions using dilute SO₂

Figure 4—The redox potential of the SO₃·⁻/SO₃²⁻ and SO₅·⁻/SO₅²⁻ couples as a function of pH (Das *et al.* 1999)

$$MnSO_4 + SO_2 + O_2 + 2H_2O \rightarrow MnO_2 + 2H_2SO_4 \quad [7]$$

$$2MnSO_4 + SO_2 + O_2 + 3H_2O \rightarrow Mn_2O_3 + 3H_2SO_4 \quad [8]$$

SO_2 can also react with O_2 to form sulphuric acid in the following side reaction:

$$SO_2 + 0.5O_2 + H_2O \rightarrow H_2SO_4 \quad [9]$$

Sulphuric acid produced by Reactions [7] to [9] can be neutralized with hydrated lime to form gypsum:

$$H_2SO_4 + Ca(OH)_2 \rightarrow CaSO_4 + 2H_2O \quad [10]$$

Experimental

Materials and apparatus

Synthetic solutions were prepared using sulphate salts of AR grade and 98% sulphuric acid. The solutions prepared resembled the solution obtained from sulphuric acid cobalt leach operations containing approximately 6.5 g/ℓ Co(II) and 2 g/ℓ Mn(II).

Laboratory tests were carried out in a 10 ℓ glass reactor fitted with baffles and a flat-blade impeller as shown in Figure 5; the solution volume for these tests was 4 l. The impeller and baffles were designed to ensure efficient mixing and consequently efficient mass transfer of the gas mixture into the liquid phase. The gases were mixed in the pipeline using a 'Venturi effect', where the smaller diameter SO₂ line was inserted such that it bends into the bigger diameter air delivery line. The SO₂ was mixed with the air in the T-piece before the gas mixture was delivered to the reactor. The gas mixture was introduced into the reactor through a glass frit located below the impeller. The temperature was controlled using a water bath, with the thermocouple positioned inside the reactor. (Figure 5.)

All tests were performed at atmospheric pressure at an impeller speed of 500 rpm. The pH and redox potential were monitored using Hamilton pH and Eh (Ag/AgCl) probes. Rotameters were used to control the SO₂ and air flow rates into the reactor while the pH was controlled by addition of 17% (w/w) hydrated lime slurry using an autotitrator connected to a peristaltic pump.

Experimental design

The experiments were designed to investigate the effects of the SO₂/air ratio, pH, temperature and the effect of using pure O₂ versus air, as indicated in Table I. One parameter was varied at a time. The same SO₂ flow rate of 11 ml/min was used in all tests. This flow rate was calculated from the stoichiometric amount of SO₂ required to precipitate 2 g/ℓ Mn(II) according to Equation [7] within a period of 5 hours. However, each test was run for 6 hours, hence some excess reagents were introduced. All tests were conducted at 30°C unless otherwise stated. (see Table I.)

Solution analysis was performed using two instruments: Varian atomic absorption spectrometer (AAS) and Varian inductively coupled plasma optical emission spectrometer (ICP-OES). Solid samples were analysed with ICP-OES, X-ray fluorescence (XRF), X-ray diffraction (XRD) and scanning electron microscopy (SEM).

Results and discussion

Effect of SO₂/air ratio

The concentration of SO₂ in the gas mixture was varied by changing the air flow rate while keeping a constant SO₂ flow rate of 11 ml/min. The various air flow rates used were; 170 ml/min, 231 ml/min, 352 ml/min, 714 ml/min, 1 439 ml/min, which were equivalent to 6%, 4.5%, 3%, 1.5% and 0.75% SO₂ (v/v) in air respectively.
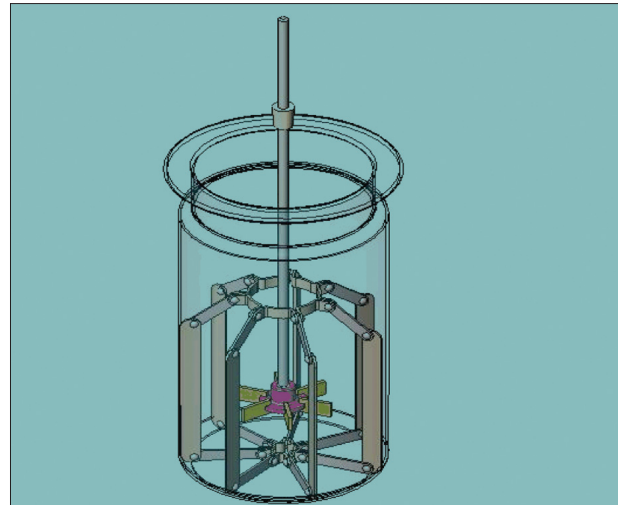

Figure 5—Reactor set-up

Table I

Experimental matrix

Parameter	Range
pH	2–4
Temperature, °C	30–60
SO₂ in air, % (v/v)	0–6
SO₂ flow rate, ml/min	11
Air flow rate, ml/min	170–1439
SO₂ in O₂, % (v/v)	3.5–23
O₂ flow rate, ml/min	36–301

Oxidative precipitation of Mn(II) from cobalt leach solutions using dilute SO_2 air

The use of SO_2/air gas mixtures resulted in faster kinetics for manganese precipitation compared to using air alone, as indicated in Figure 6. Mn precipitation increased significantly in the first 3 hours and thereafter little or no Mn precipitated further.

The extent of Mn precipitation was similar for the dilute SO_2 concentrations up to 3% SO_2 in air, which is equivalent to 13% SO_2 in O_2, as indicated in Figures 6 and 7. This SO_2/O_2 ratio is similar to the optimum of 12% SO_2 in O_2 obtained by Schulze-Messing *et al.* (2006). Menard *et al.* (2007) has, however, shown that at pH 4, Mn precipitation could still be carried out at SO_2/O_2 ratios as high as 50% if adequate mixing is provided. The high SO_2/O_2 ratios, however, result in slow kinetics compared to the low SO_2/O_2 ratios and therefore would result in longer residence times.

Zhang *et al.* (2000) reported that the optimum SO_2/O_2 ratio is O_2 mass transfer dependent, with Mn precipitation increasing with the increase in O_2 content in the gas mixture. This O_2 mass transfer dependency of the system is likely because of the large difference in the solubility of SO_2 and O_2. The slower kinetics observed at SO_2/O_2 ratios higher than the optimum can be attributed to insufficient O_2 supply in solution. Cobalt losses of 1–2% were recorded for all the SO_2/air ratios (Figure 7).

The relationship between SO_2 efficiency and lime consumption versus the SO_2/air ratio is shown in Figure 8. The efficiency of SO_2 was calculated by dividing the predicted moles of SO_2 used for Mn oxidation by the total moles of SO_2 input. The efficiency followed the same trend as Mn precipitation with maximum SO_2 efficiency recorded at 3% SO_2 in air. The total lime consumption, however, remained relatively constant, which indicated that for less oxidizing gas mixtures, the side reaction (Equation [9]) becomes dominant and consumes the SO_2 rather than Mn precipitation reaction (Equation [7]).

The relationship between the redox potential and %SO_2 in air at pH 3 is illustrated in Figure 9. The redox potential increased sharply on addition of SO_2 in air and reached a maximum potential of 1.1V vs. SHE at 3% SO_2 and decreased thereafter. It can be deduced from these results that the /air ratio controls the redox potential and therefore the oxidizing strength of the solution, and consequently the extent of Mn precipitation.
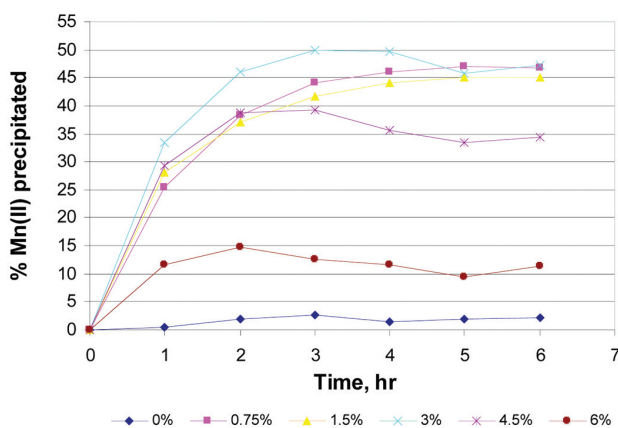
The comparative oxidizing ability of SO_2/air and SO_2/O_2 gas mixtures was investigated. The same molar quantity of O_2 was used in both instances. The extent of Mn precipitation achieved using SO_2/O_2 gas mixtures was higher than that achieved with SO_2/air gas mixtures (Figure 10). This can be attributed to the higher partial pressure of O_2 in the gas mixture and consequently higher dissolved oxygen concentration when using pure O_2 compared to air.
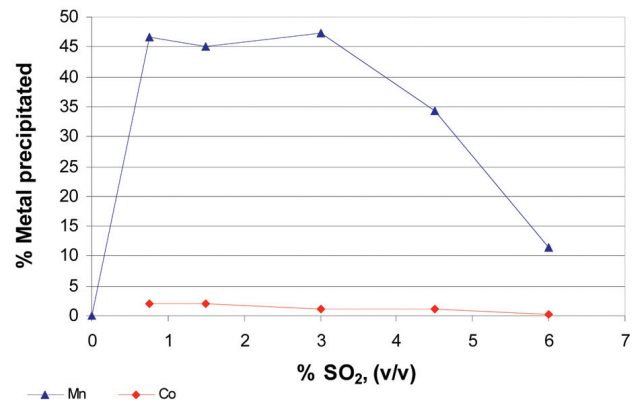

Figure 7—Effect of % SO_2 in air on Mn and Co precipitation at pH 3 (2 g/ℓ Mn(II); 6.5 g/ℓ Co(II); 30°C; 6 hours)
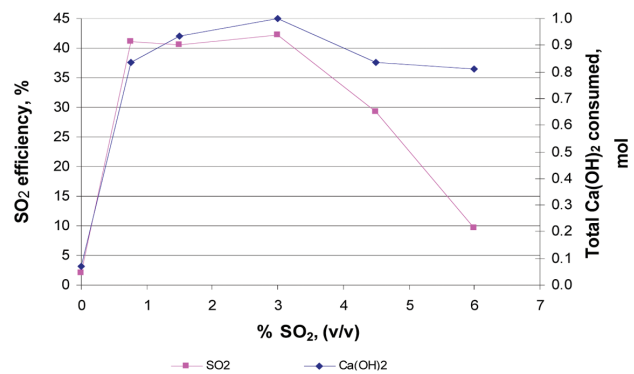

Figure 8—Effect of % SO_2 in air on SO_2 efficiency and lime consumption at pH 3 (2 g/ℓ Mn(II); 6.5 g/ℓ Co(II); 30°C; 6 hours)

Figure 6—Effect of % SO_2 in air on Mn precipitation (2 g/ℓ Mn(II); 6.5 g/ℓ Co(II); pH 3; 30°C)
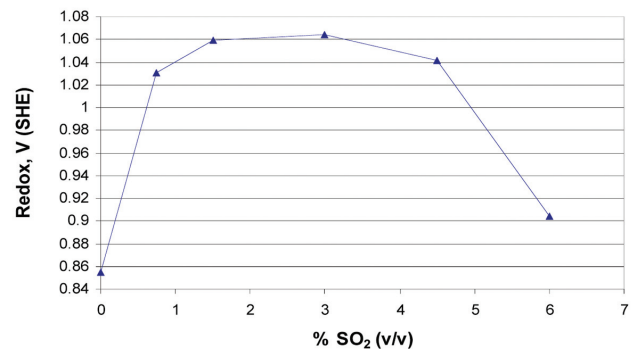

Figure 9—Effect of % SO_2 in air on the redox potential at pH 3 (2 g/ℓ Mn(II); 6.5 g/ℓ Co(II); 30°C; 6 hours)

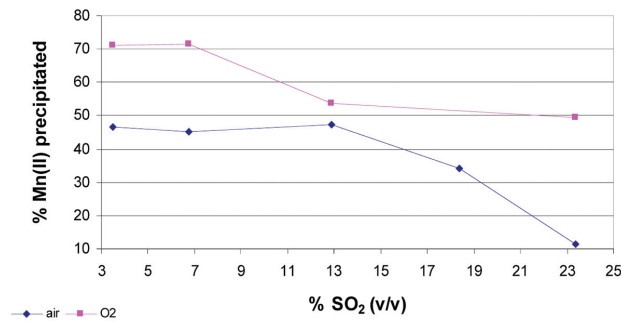# Oxidative precipitation of Mn(II) from cobalt leach solutions using dilute SO_2

Figure 10—Effect of % SO_2 in O_2 when using air and pure O_2 on Mn precipitation (2 g/ℓ Mn(II); 6.5 g/ℓ Co(II); pH 3; 30°C; 6 hours)

Effect of pH

The solution pH was varied from pH 2 to pH 4 at 30°C and 3% SO_2 in air. An increase in pH resulted in increased Mn precipitation (Figure 11). At pH 4, all Mn was precipitated from the solution after 5 hours, which represented a stoichiometric consumption of SO_2 according to Equation [7].

$$MnSO_4 + SO_2 + O_2 + 2H_2O \rightarrow MnO_2 + 2H_2SO_4 \quad [7]$$
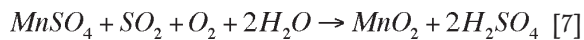
An increase in pH also resulted in increased Mn and Co precipitation, as illustrated in Figure 12. Mn and Co precipitation was relatively constant at pH values less than 3, but a sharp increase in precipitation of both metals was observed at pH values above pH 3, as indicated in Figure 12. Zhang *et al*. (2002) also found the extent of Mn precipitation at pH values less than 3 to be slow; but as pH increased above pH 4, the rate of Mn precipitation became fast. It appears from these results that Mn and Co precipitation is relatively independent of pH at pH values less than 3. A cobalt loss of 1% was recorded at pH 3 and the cobalt loss increased linearly as pH was increased from pH 3 to pH 4. The higher cobalt losses recorded at higher pH values are possibly due to higher Mn removal at those pH values, which results in the presence of excess oxidant in solution, which consequently oxidizes the Co(II). Therefore Co losses at higher pH values can be limited by stopping the process as soon as sufficient Mn has been removed from solution.

The marked increase in Mn and Co precipitation at pH values above pH 3 shows the strong influence of pH on the SO_2/O_2 system, as already reported by other authors (Menard *et al*. 2007; Zhang *et al*. 2000). The increase in Mn precipitation at pH values above pH 3 could be attributed to a change in the speciation of the S(IV) species (Figure 2) as both Co(II) and Mn(II) are expected to remain in solution in the pH range of pH 2 to pH 4 (Figure 1).

From the S(IV) speciation diagram (Figure 2), it is observed that at pH 2 the $SO_2.H_2O$ and HSO_3^- species are equally dominant, but as pH increases from pH 2 to pH 4, HSO_3^- becomes the dominant S(IV) species. It has been reported that the HSO_3^- species is 53 times more reactive than the $SO_2.H_2O$ species for the oxidation of S(IV) (Brandt *et al*. 1994). Consequently, an increase in Mn and Co precipitation at pH values above 3 was possibly due to improved kinetics caused by an increase in dominance of the more reactive HSO_3^- species over the $SO_2.H_2O$ species as pH was increased.

Figure 13 shows the effect of pH on Mn precipitation as well as redox potential for 3% SO_2 in air. The redox potential decreased linearly as the pH increased but Mn precipitation increased significantly, at pH values greater than 3. The redox potential followed the same trend observed for the sulphite radical couples indicated in Figure 4. From these results it appears that the redox potential alone is not responsible for the oxidative precipitation of Mn since only half of Mn(II) was removed at the high redox potentials measured at pH 2 to pH 3, whereas 100% Mn(II) removal was achieved at the lower redox potential measured at pH 4.
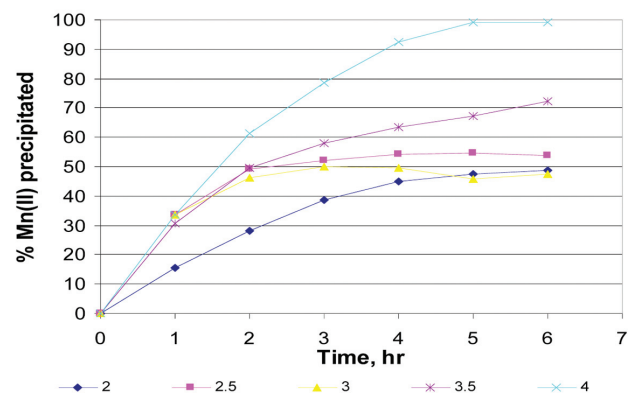

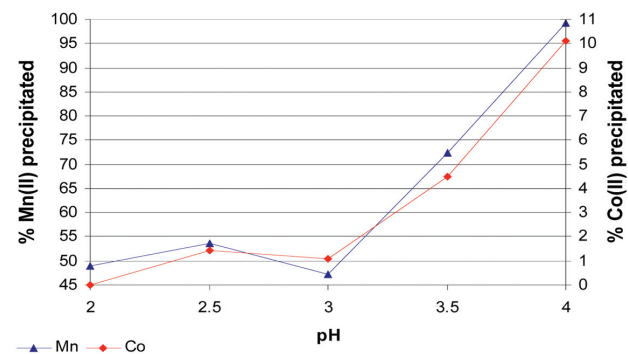**Figure 11—Effect of pH on Mn precipitation (2 g/ℓ Mn(II); 6.5 g/ℓ Co(II); 3% SO_2 in air; 30°C)**

Figure 12—Effect of pH on Mn and Co precipitation for 3% SO_2 in air (2 g/ℓ Mn(II); 6.5 g/ℓ Co(II); 30°C; 6 hours)
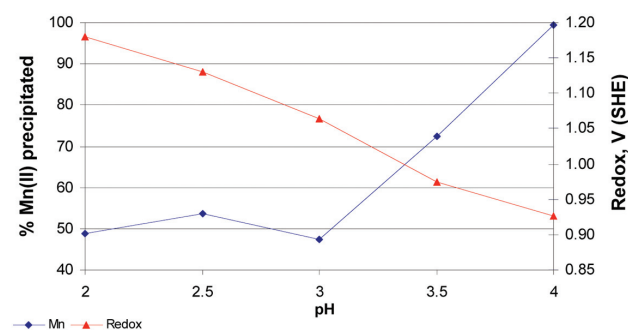

Figure 13—Effect of pH on Mn precipitation and redox potential at 3% SO_2 (2 g/ℓ Mn(II); 6.5 g/ℓ Co(II); 30°C; 6 hours)

Oxidative precipitation of Mn(II) from cobalt leach solutions using dilute SO_2 air

Figure 14 shows the redox potential measured for the 3% SO_2/air gas mixture and the redox potential measured when using O_2 alone. The MnO_2/Mn(II) line and the Co_3O_4/Co(II) lines predicted by the HSC model in Figure 1 were also superimposed on the diagram.

Although the redox potentials measured for O_2 followed a similar trend as the SO_2/air gas mixture, the extent of Mn precipitation by O_2 alone was negligible (0.2%), compared to the extent of Mn precipitation by the 3% SO_2/air gas mixture (50%). It can also be observed from Figure 14 that the redox potential values measured for the 3% SO_2/air gas mixture and O_2 alone at various pH values lie within the (MnO_2 + Co(II)) region in the Pourbaix diagram. Hence, thermodynamically, MnO_2 is expected to precipitate from pH 2 to pH 4, as it was the case for the 3% SO_2/air gas mixture; however, it was not the case for the O_2 gas. These results further highlight that high redox potential values alone are not responsible for the precipitation of Mn, but the presence of reactive S(IV) species, which are responsible for the radical mechanism, is probably required for Mn precipitation. The fact that Mn precipitation increased significantly at pH values above pH 3 even though the measured redox for all the pH values lies within the MnO_2 predominance region, further emphasizses the dependence of the kinetics on the S(IV) speciation.

From Figure 14 the measured redox potential crossed into the Co_3O_4 predominance region only at pH 3.5, which indicates that cobalt oxidative co-precipitation is thermodynamically feasible at pH 3.5 and higher. Only 1% cobalt was lost at pH 3.

Effect of temperature

The effect of temperature was investigated by varying the solution temperature from 30°C to 60°C at pH 3 and 3% SO_2 as indicated in Figure 15. The extent of Mn and Co precipitation increased linearly with increasing temperature. The increase in the rate of reactions upon increasing the temperature was expected due to the temperature dependence of reaction kinetics. Complete Mn precipitation was achieved at 50°C but at a cobalt loss of 17%. The high cobalt loss could be due to the fact that all the Mn had been precipitated within this period, leaving the oxidant free to oxidize the Co(II) in solution.

An activation energy of 25 kJ/mol was calculated from the Arrhenius plot at pH 3 and 3% SO_2. This activation energy is similar to the value of 23.5 kJ/mol obtained by Schulze Messing *et al.* (2007). The activation energy calculated for these conditions lies between 20 and 40 kJ/mol, which indicates that Mn precipitation is under mixed reaction control and that O_2 mass transfer is most likely the dominant limiting factor compared to slow chemical reaction steps. The dominance of mass transfer reaction control can be supported by the large difference in the solubility of SO_2 compared to O_2 as well as the increase in Mn precipitation observed when the quantity of O_2 in the SO_2/air and SO_2/O_2 gas mixture was increased.

Precipitation product

The precipitate was analysed using ICP-OES, SEM, XRF and XRD techniques. The XRD results indicated that the precipitate consisted mostly of gypsum ($CaSO_4$), bassanite ($CaSO_4$.xH_2O), calcite (CaO) and bixbyite (Mn^{3+},Fe^{3+})$_2O_3$.

According to the XRD analysis, Mn precipitated in the form of Mn_2O_3 and not MnO_2 as predicted from the thermodynamic data. The reason for this is still under investigation. The SEM micrographs in Figures 16 and 17 indicate the two phases that were present in the precipitate. The major phase in the precipitate contained $CaSO_4$ (99%), which is represented by the white areas in Figure 16. The manganese precipitate phase (< 1%) is the bright white spot indicated by the arrow in Figure 17. The cobalt that co-precipitated reported to the manganese precipitate phase as indicated by the X-ray scan in Figure 17.

Conclusions

Precipitation of Mn with SO_2/air gas mixtures resulted in higher Mn removal compared to using air or oxygen alone. The use of pure O_2 instead of air in the SO_2 gas mixtures also resulted in improved Mn precipitation. Solution pH was found to play a major role in the precipitation reactions and the rate of Mn precipitation increased significantly only at pH values above 3. The SO_2 concentration in the gas mixture was found to control the redox potential of the system and therefore the oxidizing strength of the solution to oxidatively precipitate Mn. The oxidizing strength of the solution decreased at SO_2/air ratios higher than 3% SO_2, which is equivalent to 13% SO_2 in O_2. The efficiency of SO_2 use for Mn(II) precipitation also followed the same trend as the extent of Mn precipitation; however, lime consumption did not decrease
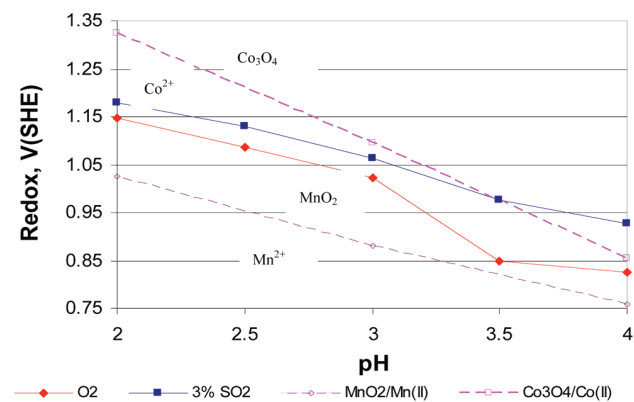

Figure 14—Effect of pH on the measured redox potential for O_2 at 700 ml/min and 3% SO_2 in air at 362 ml/min (2 g/ℓ Mn(II); 6.5 g/ℓ Co(II); pH 3, 30°C, 6 hours)
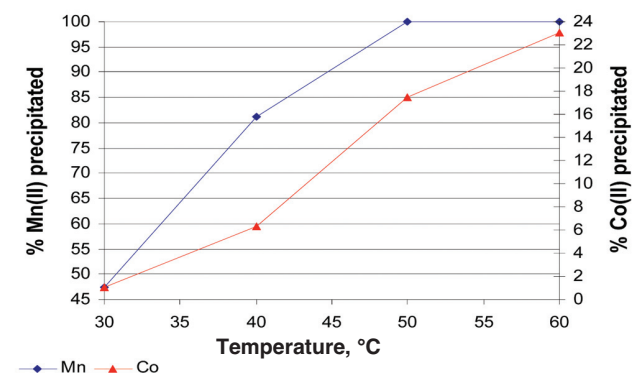

Figure 15—Effect of temperature on Mn precipitation (6.5 g/ℓ Co(II); 2 g/ℓ Mn(II); pH 3; 3% SO_2; 6 hours)

Oxidative precipitation of Mn(II) from cobalt leach solutions using dilute SO_2
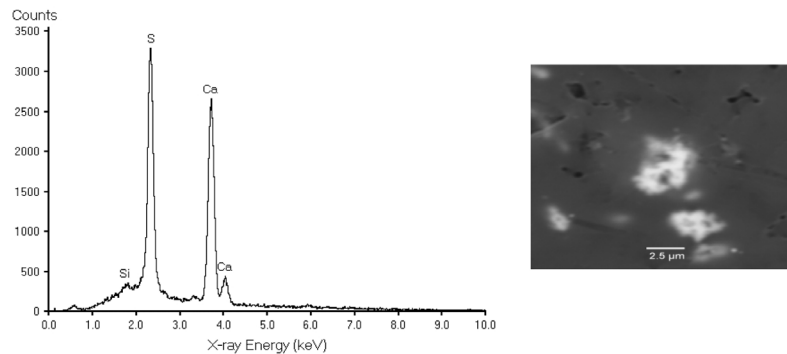

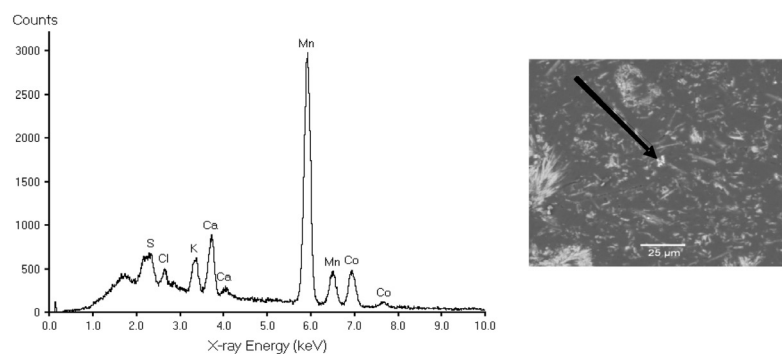Figure 16—The SEM micrograph for the $CaSO_4$ phase

Figure 17—The SEM micrograph for the Mn precipitate phase

significantly at SO_2/air ratios > 3%, which indicates that the SO_2 was mainly consumed by the side reaction of sulphuric acid production.

An increase in temperature resulted in both increased Mn precipitation and cobalt co-precipitation. An activation energy of 25 kJ/mol was calculated from the Arrhenius plot at 3% SO_2 and pH 3; which indicates that at these conditions, the reactions are both diffusion and chemically controlled. Diffusion control could be more limiting given the possible O_2 mass transfer limitation.

Although pure O_2 resulted in similar measured redox potentials compared to the 3% SO_2/air gas mixtures at pH 3, the extent of Mn precipitation with pure O_2 was insignificant compared to the extent of Mn precipitation by the 3% SO_2/air gas mixture. It was evident from these results that high redox potential values alone are not responsible for Mn precipitation and that S(IV) species play an important role in the mechanism of Mn precipitation with SO_2/air gas mixtures. Therefore the reaction mechanism is possibly governed by both pH and redox potential, depending on the oxidizing ability of the gas mixture. However, pH and consequently the reactivity of the S(IV) species, had the most pronounced effect on the Mn precipitation reactions.

XRD and SEM analysis revealed that the precipitate produced consisted mainly of gypsum or bassanite (99%), with the Mn containing phase (< 1%) distributed within the gypsum phase. The co-precipitated cobalt reported to the manganese phase. The manganese precipitate was found to be in the form of Mn_2O_3 rather than MnO_2.

References

1. BERGLUND, J. and ELDING, L.I. Reaction of peroxomonosulphate radical with manganese(II) in acidic aqueous solution, *Journal of Chemical Society Faraday Transactions*, vol. 90, no. 21, 1994. pp. 3309–3313.
2. BRANDT, C. and VAN ELDIK, R. Transition metal-catalysed oxidation of sulphur(IV) oxides. Atmospheric relevant processes and mechanisms, *Chemical Review*, vol. 95, 1995. 1994. pp. 119–190.
3. DAS, N.T., HUIE, R.E., and NETA, P. Reduction potentials of $SO_3^{\cdot-}$, $SO_5^{\cdot-}$ and $S_4O_6^{\cdot3-}$ radicals in aqueous solution, *Journal of Physical chemistry*, vol. 103, 1999. pp. 358–3588.
4. HUIE, R.E. and NETA, P. *Journal of Atmospheric Environment*, vol. 21, 1987. p. 1743.
5. MENARD, V. and DEMOPOULOS, G.P. Gas transfer kinetics and redox potential considerations in oxidative precipitation of manganese from an industrial zinc sulphate solution with SO_2/O_2, *Hydrometallurgy*, vol. 89, 2007. pp. 357–368.
6. SCHULZE-MESSING, J. ALEXANDER, D.C., SOLE, K.C., STEYL, J.D.T., NICOL, M.J., and GAYLARD, P. An Empirical Rate Equation for the Partial Removal of Manganese from Solution using a Gas Mixture of Sulphur Dioxide and Oxygen, *Hydrometallurgy*, vol. 86, 2007. pp, 37–43.
7. ZHANG, W., SINGH, P., and MUIR, D.M. SO_2/O_2 as an oxidant in hydrometallurgy, *Minerals Engineering*, vol. 13, 2000. pp. 1319–1328.
8. ZHANG, W., SINGH, P., and MUIR, D.M. Oxidative precipitation of manganese with SO_2/O_2 and separation from cobalt and nickel, *Hydrometallurgy*, vol. 63, 2002. pp. 127–135.
9. ZHANG, W. and CHENG, C.Y. Manganese metallurgy review. Part III: Manganese control in zinc and copper electrolytes, *Hydrometallurgy*, vol. 89, 2007. pp. 178–188. ◆